

## **A Glassy Lowermost Outer Core**

**Vernon F. Cormier**

University of Connecticut, Physics Department, 2152 Hillside Road, Storrs, CT 06269-3046, USA

### **SUMMARY**

New theories for the viscosity of metallic melts at core pressures and temperatures, together with observations of translational modes of oscillation of the Earth's solid inner core, have proposed that the dynamic viscosity of Earth's liquid outer core may approach  $10^{11}$  Pa-sec near the inner core boundary. If the viscosity of the lowermost outer core (F region) were in this range, it may be in a glassy state, characterized by a frequency dependent shear modulus and increased viscoelastic attenuation. Testing this hypothesis, the amplitudes of high frequency PKiKP waves are found to be consistent with an upper bound to shear velocity in the lowermost outer core of 0.5 km/sec at 1Hz. Fitting a Maxwell rheology for the frequency dependent shear modulus to seismic constraints at both low and high frequency results in a model of the F region as a 400 km thick chemical boundary layer. This layer likely has both a higher density and higher viscosity than bulk of the outer core, with a peak viscosity on the order of  $10^9$  Pa-sec or higher near the inner core boundary. If lateral variations in the F region are confirmed to correlate with lateral variations observed in the structure of the upper most inner core, they may be used to map differences in the solidification process of the inner core and flow in the lowermost outer core.

Key words: composition of the core, viscosity, seismic body waves

AGU Index terms: 1015 Composition of the core, 1507 Core processes, 7203 Body waves, 7207 Core

## 1 INTRODUCTION

The value of viscosity of Earth's liquid outer core is important to in controlling the behavior of fluid motions that drive the geodynamo, including its turbulence as a function of depth. Brazkin and Lyapin (2000) have recently questioned the validity of the Arrhenius rate-activated model of viscosity at the pressures of planetary and stellar cores and suggested a strong pressure dependence of the dynamic viscosity of metallic liquids. This suggestion together with a reported observation of the translational (Slichter) modes of the inner core have led Smylie et al. (2009) to estimate a viscosity of  $1.2 \times 10^{11}$  Pa-sec near the inner core boundary with log-linear increase from a value of 2.4 Pa-sec near the core-mantle boundary. These high viscosity estimates are in stark contrast to the value of  $1.5 \times 10^{-2}$  Pa-sec obtained by de Wijs et al. (1998) from ab initio calculations for iron alloys at core pressures and temperatures.

A material having a viscosity as high as  $10^{11}$  Pa-sec will exhibit a frequency dependent shear modulus whose effects may be observable in seismic wavefields sampling the liquid outer core near the solid inner core boundary. Materials exhibiting this behavior are loosely termed "glassy" in the sense that their molecular and atomic structures are amorphous like that of true liquids but are solid in the sense that they have a non-zero shear modulus. A material in a glassy state, however, is not strictly a true glass, which is identified by a phase transition associated with a second order discontinuity in the phase diagrams of the bulk and shear moduli, e.g., Zhang et al. (2007).

Independent of viscosity estimates, another clue to the existence of a glassy state of the lowermost outer core are observations of anomalous splitting Earth's free oscillations. From fits to the spheroidal mode  ${}_2S_3$ , Tsuboi and Saito (2002) have proposed the existence of a 40 km thick zone of non-zero shear modulus above the inner core boundary. Their mode fit required a shear velocity of 0.017 km/sec at 0.001 Hz in this zone.

A simple theory for the frequency dependence of the shear modulus of a high viscosity fluid can be applied as a check on the possibility of a glassy state in the lowermost outer core. This paper applies this theory to extrapolate estimates of shear modulus in this region from observations in the frequency band of Earth's solid tides and free oscillations to observations in the band of high frequency (1 Hz) body waves. Upper bounds are obtained on the 1 Hz shear modulus and dynamic viscosity in the lowermost outer core from the amplitudes of body waves reflected by and diffracted along the boundary of solid inner core.

## 2 RHEOLOGY

The rheology assumed for the frequency dependent shear modulus is that of a simple Maxwell fluid:

$$(1) \quad \mu(\omega) = \frac{\mu_\infty i \omega \tau_R}{1 + i \omega \tau_R}$$

(e.g., Wilhelm et al., 2002), where  $\mu_\infty$  is the shear modulus at infinite frequency and  $\tau_R$  is a relaxation time given by the ratio of viscosity  $\eta$  to  $\mu_\infty$ , i.e.,

$$(2) \quad \tau_R = \frac{\eta}{\mu_\infty} .$$

From the frequency dependent, complex, shear modulus of eq. (1), a real frequency dependent shear velocity can be defined from

$$(3) \quad \beta(\omega) = \text{Re} \left( \sqrt{\frac{\mu(\omega)}{\rho}} \right) ,$$

and a frequency dependent shear wave attenuation from

$$(4) \quad Q_\beta^{-1} = \frac{2 \text{Im}[\mu(\omega)]}{\text{Re}[\mu(\omega)]} .$$

If the bulk attenuation of the fluid is neglectibly smaller than the shear attenuation, the attenuation of a compressional wave in the viscous fluid is related to the shear attenuation by

$$(5) \quad Q_\alpha^{-1} = (4/3) \left( \frac{\beta}{\alpha} \right)^2 Q_\beta^{-1} ,$$

(Anderson, 1989). The predictions of eqs. (3) and (5) for the frequency dependent S wave velocity and P wave attenuation at the base of the mantle can be tested against seismic observations in different frequency bands to determine constraints on viscosity.

A limiting assumption of the simple rheology given by eqs (1) and (2) is that stress relaxation occurs at a single time rather than a spectrum of times, which might be a more realistic for the chemistry of a metal alloy. Experimental work with metallic glasses has found that a rheology specified by a complex compliance (the reciprocal of complex modulus) better characterizes the flow characteristics of the rheology (Schroter et al., 1998).

## 3 SEISMIC OBSERVATIONS AND MODELING

### 3.1 Free-Oscillations

Sato (1964) noted that a small non-zero shear modulus throughout the outer core would have negligible effect on most of Earth's eigenfrequencies and produce a "soft core" splitting that might be observed in some core-sensitive modes. Expanding on this idea, Tsuboi and Saito (2002) called attention to problems that remain in fitting the observed splitting of core-sensitive modes that cannot be satisfied by models of inner core anisotropy. They calculated the soft-core splitting of the spheroidal mode  ${}_3S_2$  for models having a non-zero shear modulus near the bottom of the outer core and were able to fit the observed splitting with a 40 km thick region above the inner core boundary in which the shear velocity was 0.0015 km/sec. Since Tsuboi and Saito's prediction, the splitting of  ${}_3S_2$  has not been revisited by any researcher.

### 3.2 Slichter Mode

The Slichter (1961) mode represents the translational oscillation Earth's solid inner core within its liquid outer core, and is identified as  ${}_1S_1$ . Intuitively one would expect that the damping of the Slichter mode would be strongly affected by the viscosity of the liquid outer core surrounding the inner core boundary. From a VLBI identification of the Slichter mode Palmer and Smylie (1995) estimated a viscosity of  $6 \times 10^2$  Pa-sec at the top of the outer core, or 5 orders of magnitude higher than the prediction of deWijfs et al. (1998). Later Smylie (1999) estimated a viscosity of  $1.2 \times 10^{11}$  Pa-sec at the bottom of the outer core from the damping of the Slichter mode. The specific observation used in his estimate was the splitting or difference in the eigenfrequencies of the translational oscillation in two orthogonal equatorial directions. Both the observations and computations of the Slichter mode eigenfrequencies, however, have a long history of uncertainty and debate. From superconducting gravimeters, Smylie's observations of two Slichter modes were 0.077 and 0.069 Mhz, but from strain records of the great 2004 Sumatra earthquake, Okubo (2009) determined the eigenfrequencies of two Slichter modes to be 0.057 Mhz and 0.051 Mhz.

### 3.3 Body Waves

At the high frequency end of teleseismic data (0.2 to 2 Hz.), body waves can provide constraints on the shear modulus and attenuation in the lowermost outer core and, combined with low frequency observations and the rheology of eq. (1), its viscosity. Compressional body waves interact with the inner core boundary region over a wide range of angles of incidence, each range having a different amount of sensitivity to the shear modulus and attenuation in the lowermost outer core. The following subsections review the constraints in over a broad range of angle of incidence, starting from near vertical to grazing incidence on the inner core boundary (ICB).

### 3.3.1 PKiKP amplitudes

At near vertical incidence on the inner core boundary, the amplitude of the PKiKP wave should be nearly insensitive to the shear velocity contrast at the inner core boundary, since no converted or reflected shear waves can be excited at vertical incidence. At vertical incidence, its reflection coefficient is a function only of the P velocity and density on either side of the ICB. Hence, if the P wave velocity is well known on either side of the ICB from travel time inversions, then the amplitude of PKiKP at near vertical incidence can be used to measure the density contrast at the inner core boundary. A disappointing limitation to this possibility is that all other effects on the PKiKP must be well known, including source radiation pattern, source-spectrum, viscoelastic and scattering attenuation, and geometric spreading in a 3-D Earth. Since the paths of PKiKP and PcP are nearly the same near the source and in the upper mantle, many of these effects are eliminated or minimized by studying the amplitude ratio PKiKP/PcP (Figure 1), still leaving strong effects due to the path differences of PKiKP and PKiKP sampling lateral variations near the core-mantle boundary. Within the uncertainties of PKiKP/PcP ratios, either a completely rigid or completely liquid lowermost outer core, can fit observations based on a standard earth model within error bars in the great circle distance range 0 to 20°.

At longer ranges and larger angles of incidence on the ICB, PKiKP amplitudes become more sensitive to the shear velocity discontinuity the shear velocity on the liquid side of the ICB. PcP amplitudes, however, become too small to rise above noise to use the PKiKP/PcP amplitude ratio to remove effects of the source mechanism and the heterogeneous structure of the upper mantle and crust. Krasnocheskov et al. (2005) measured absolute PKiKP amplitudes in the great circle range up to 100°, finding that observed amplitudes could near 50° to 100° could not be fit with standard earth models of the ICB region (Figure 2). Krasnocheskov et al.'s measures of absolute PKiKP amplitudes were obtained from PKiKP waveforms stacked from arrays of different nuclear explosions at known locations around major test sites, normalizing source strength to a fixed explosive yield. Assuming that each explosion does not strongly deviate from a fixed spectral shape and radiation pattern, then one possible model of the ICB boundary region that fits observations is a model in which the liquid outer core near the ICB has a shear velocity of 0.5 km/sec.

The curves shown in Figure 2 were obtained from measuring peak to peak amplitudes of PKiKP particle velocity in a narrow band around 1 Hz, synthesized by a full-wave code utilizing ray-parameter integration (Cormier and Richards, 1989). Depending on the frequency content of the assumed source spectrum and the mantle attenuation model, some smoothing over the zeros in the PKiKP reflection coefficient in the 50° to 100° range was observed in computational experiments. For the likely frequency content of Krasnocheskov's data, however, this smoothing effect was not sufficient to explain the higher amplitudes of the data in this range compared to prediction of a standard Earth model having a zero modulus at the bottom of the outer core.

Now, assuming a shear velocity at 1 Hz of 0.5 km/sec from Kransocheskov et al.'s PKiKP observations and a shear velocity at 0.001 Hz of 0.0015 km/sec from Tsuboi and Saito's estimate from the splitting of the  ${}_2S_3$ , a viscosity of  $10^9$  Pa-sec can be estimated from the frequency dependent shear modulus and its relation to viscosity given by eqs. (1) and (3). Figure 3 shows how the extrapolated frequency dependence of shear velocity may connect these estimates of shear velocity of 0.0015 km/sec at 0.001 and to a shear velocity of 0.5 km/sec at 1 Hz. The fit between 0.001 Hz and 1 Hz with this model requires a unrelaxed shear velocity of 1.2 km/sec as frequency approaches infinity. In the range of 2 to 5 Hz, the highest frequency band commonly observable above noise in teleseismic data, the predicted shear velocity is approximately 1 km/sec.

Alternatively, assuming the correctness Smylie et al.'s viscosity estimate of  $1.2 \times 10^{11}$  Pa-sec and a shear velocity at 1 Hz of 0.5 km/sec, eqs. (1) and (3) can be used to extrapolate the shear modulus to the free oscillation frequency band. This extrapolation leads to an estimate of shear velocity of 0.144 km/sec at 0.001 Hz. This is the lowest possible shear velocity at 0.001 Hz obtainable with the rheology of eqs (1) and (3), a factor of 1000 times Tsuboi and Saito's estimate of 0.0015 km/sec. In this model, the shear velocity at 1 Hz is close to its unrelaxed, infinite frequency, limit of 0.5 km/sec.

### 3.3.2 PKP-Cdiff amplitudes

The path of the compressional wave that diffracts around the ICB (PKP-Cdiff) spends a long time in the lowermost outer core. It should be especially sensitive to the viscoelastic attenuation of the region, apart from any sensitivity it may have to velocity and density contrasts across the ICB. The  $10^9$  viscosity model and the  $10^{11}$  viscosity model predict very different attenuation at 1 Hz (Figure 4). At 1 Hz the  $10^9$  viscosity model predicts a  $Q = 170$  and the  $10^{11}$  viscosity model  $Q = 22,000$ . From spectral ratios of compressional waves with long residence times in the outer core, e.g., PK7KP/PK4KP, Cormier and Richards (1976) estimate a lower bound to  $Q_k$  in the outer core of 10,000. Since the rays of PKnKP waves turn in the middle of the outer core, these observations do not preclude the possibility of strong increase in attenuation (strong decrease in  $Q$ ) near the inner core boundary. Such a low  $Q$  zone may be detected by the amplitude and frequency content of compressional waves diffracted around the inner core, making it possible to discriminate between the  $10^9$  and  $10^{11}$  viscosity models.

Figure 5 shows the effects of a non-zero rigidity in the lowermost outer core on compressional waves interacting with the ICB. These profiles are synthesized and filtered with procedures identical to those described in the study of Zou et al. (2008). That study modeled the amplitude decay of PKP-Cdiff and the difference in travel time between PKiKP and PKP-Cdiff to constrain the velocity and attenuation profiles in the lowermost outer core. Even with a shear velocity as high as that of the solid inner core ( $V_s = 3.5$  km/sec), the effects on compressional waves interacting with the inner core are small in Figure 5. A rigid lowermost outer core predicts a barely perceptibly smaller PKP-Cdiff wave and a barely perceptibly larger PKiIKP wave (a compressional wave reflected once from the underside of the inner core). With non-zero rigidity in the

lowermost outer core, the underside ICB reflection is enhanced due to the fact that less energy is partitioned into P converted S energy in the solid inner core (smaller PKJKP wave).

Figure 6 compares measured PKIKP/PKP-Cdiff amplitude ratios with those predicted for seismograms synthesized in different models of P and S velocity profiles in the lowermost outer core. An extensive modeling effort considering just the effects of P velocity gradient and attenuation on the outer core side of the ICB is described in Zou et al. (2008). The supplement to that study shown here includes the results of additional experiments that varied the shear velocity the outer core side of the ICB. Models PREM (Dziewonski and Anderson, 1981) and PREM2 (Song and Helmberger, 19xx) bound the scatter in the observed amplitude ratio. Compared to PREM, PREM2 has reduced K velocity gradient at the bottom of the outer core (Figure 7). The effect of a non-zero rigidity on the outer core side of the ICB is to lower the PKIKP/Cdiff amplitude ratio. Even in the extreme case of shear velocity equal to that on the solid inner core side of the boundary (PREM2-R vs PREM2 in Figure 6), however, the effect would hardly be a useful diagnostic of a glassy lowermost outer core given the observed scatter in the amplitude ratio. Some of the variance in the observed amplitude ratio scatter might be due to lateral variation in viscoelastic and scattering properties of the inner core sampled by the PKIKP phase in the ratio. These lateral variations in the structure of the uppermost inner core are now well documented in many studies (e.g., Stroujkova and Cormier, 2004; Yu et al., 2005, Leyton and Koper, 2007).

The Zou et al. study had difficulty in simultaneously fitting the observed PKP-Cdiff/PKIKP amplitude ratio and the travel time difference between PKIKP and PKP-Cdiff, finding that a PREM (Dziewonski and Anderson, 1991) model best fit the amplitude ratios but a PREM2 (Song and Helmberger, 1995) type model best fit the differential travel times. They found that only by introducing some compressional wave attenuation in the lowermost outer core could a PREM2 type model could fit the amplitude ratio. Their preferred mechanisms of attenuation consisted of either the effects of volumetric scattering in a slurry zone, scattering by ICB topography, or a viscoelastic  $Q = 300$  in the lowermost 350 km of the outer core. Any viscoelastic  $Q$  in the lowermost outer core smaller than this value would conflict with the amplitudes of high frequency PKiKP + PKIKP waves observed in the  $110^\circ$  to  $130^\circ$  range (Cormier 1981). If viscoelasticity in the lowermost outer core is the correct attenuation mechanism to explain PKP-Cdiff amplitudes, then this would favor the  $10^9$  Pa-sec viscosity model of the of the lowermost outer core, which predicts a  $Q$  of 450 in the narrow band around 0.3 Hz of Zou et al.'s study. This estimate assumes that the attenuation is primarily in shear and that an associated bulk attenuation of the type described by Stevenson (1983) is much smaller. Thus, it would seem that combined travel time and amplitude behavior of PKP-Cdiff favor the  $10^9$  Pa-sec viscosity model. The supplemental study shown here, however, found that it may still be possible to achieve a fit to both differential travel times and the PKP-Cdiff/PKIKP amplitude ratio by modifying the velocity profile alone in the lowermost mantle without either a zone of high attenuation or non-zero rigidity in the "Best Fit" labeled curves in Figures 6 and 7. The Best Fit labeled model has a PREM

type gradient in compressional wave velocity of  $0.0005 \text{ sec}^{-1}$  above the ICB and a PREM2 type P velocity jump at the ICB.

#### 4 DISCUSSION

If the viscosity of the lowermost outer core is  $10^9$  Pa-sec or higher and its composition is assumed to be nearly uniform and equal to that of the entire outer core, then the P wave velocity should exhibit an increase or increased positive gradient with depth since

$$V_p = \sqrt{\frac{K + 4/3 \mu}{\rho}} .$$
 With increased viscosity implying a non-zero, frequency

dependent shear modulus  $\mu$ , the P velocity will increase at a faster rate with depth in this region. With the increased shear modulus there might also be an associated smaller increase in bulk modulus. Unless the chemistry also changes in this region such that density increases, a viscosity increase near the inner core boundary would thus predict travel times of compressional waves at grazing incidence to the inner core that disagree with the predictions of all recent models of compressional velocity near the inner core boundary, including PREM2, AK135, and IASP91. It is important here to note that PREM2, AK135, and IASP91, unlike PREM, all contain significant constraints from picking and interpreting travel times from distances  $110^\circ$  to  $150^\circ$ , where the multi-branched region of the travel times of core waves had previously made bulletin reported travel times unreliable at the time PREM was constructed. Earth models constrained by more complete sets of core travel times all suggest that the reduced P velocity gradient in the lowermost core is nearly global feature. Its existence may signify a region that is denser and chemically distinct from the region of the outer core above it. From the reduced velocity gradient in this region common to many recent standard models, Gubbins et al. (2008) have suggested it to be a thermochemical boundary layer. They propose that the composition changes continuously toward the composition of the solid inner core, with the integrated density increase in this layer being added to the density discontinuity at the ICB needed to drive the geodynamo by compositional convection.

The long term persistence of this structural feature beneath a vigorously convecting outer core having velocities on the order of kilometers per year may itself suggest that its viscosity is much higher than the region above it. Likewise any evidence of lateral variations in its structure may also suggest higher viscosity, since these lateral variations would tend to be erased by convection in the outer core. Yu et al. (2005) find evidence that the velocity gradient at the bottom of the outer core is more PREM-like in the quasi-equatorial eastern hemisphere and more PREM2/AK135/IASP91-like in the equatorial western hemisphere. Like the quasi-hemispherical variations in anisotropy, attenuation, and scattering found in the uppermost solid inner core, variations in viscosity structure near the bottom of the outer core may record lateral variations both in the processes of inner core solidification (Bergman, 2005; Cormier, 2007) and as well as lateral large scale flow at the bottom of the outer (Aubert et al., 2008).

The high viscosity at the bottom of the outer core suggested by seismic data are not in conflict with the results of numerical dynamo modeling. A key parameter controlling the

spatial spectrum of the magnetic field and its dipole stability and reversal frequency is the Ekman number  $E$ :

$$E = \frac{\eta}{\rho \Omega L^2},$$

where  $\eta$  is the dynamic viscosity,  $\rho$  density,  $\Omega$  Earth's angular rotation velocity, and  $L$  the thickness of Earth's liquid outer core. The common assumption is for  $\eta$  to be on the order of de Wijs's et al's  $\eta$  estimate, which gives  $E = 10^{-15}$ . This Ekman regime, however, is numerically inaccessible within the limitations of numerical modeling. The majority of numerical geodynamo calculations performed thus far are confined to the regime  $E \geq 10^{-6}$  (e.g., the review by Rudiger and Hollerbach, 2004). The severity of this limitation is lessened by the fact that the smallest scales of spatial variation of the magnetic field controlled by a low Ekman number are unobservable at the Earth's surface. For a dynamic viscosity  $10^9$  Pa-sec, the Ekman number is  $10^{-4}$  in the lowermost mantle, which is still within the explored domain of many numerical geodynamo simulations. Even at the highest viscosity of  $10^{11}$  Pa-sec suggested by seismic observations, it is important to emphasize that seismic data suggest that these high viscosities may exist only the lowermost 40 to 400 km of Earth's outer core, with the rest of the outer core characterized viscosities possibly as low as those estimated by de Wijs et al., with the corresponding Ekman numbers likely to be in the range  $10^{-6}$  to  $10^{-15}$  throughout most of the volume of the outer core.

## 5 CONCLUSIONS

Seismic data in a frequency band ranging from the  $5 \times 10^{-5}$  Hz to 1 Hz suggest that the lowermost 40 to 400 km of Earth's outer core is characterized by a strong increase in viscosity, which may be high enough to exhibit a frequency dependent shear modulus. A viscosity of  $10^9$  Pa-sec near the inner core boundary is the most consistent with the broad band of seismic observations, ranging from the periods and damping of the Slichter mode, the splitting of the spheroidal mode  ${}_2S_3$ , the amplitude of PKiKP in the  $40^\circ$  to  $90^\circ$  range, and the travel time and distance decay of PKP-Cdiff. PKiKP amplitudes are consistent with an upper bound of 1 Hz shear wave velocity of 0.5 km/sec and an upper bound to viscosity of  $10^{11}$  Pa-sec. Each of the seismic observations, however, is challenging, requiring measurement of small and subtle features of data. Multiple, reproducible, detections and measurement of the Slichter mode have yet to occur. The splitting of  ${}_2S_3$  is a feature of the free oscillation spectrum that can be affected by anisotropic and laterally heterogeneous structure in the solid inner core as well as laterally heterogeneous structure at the bottom of the liquid outer core. The measurement of the absolute amplitude of high frequency PKiKP in the region of the zeros in the ICB reflection coefficient requires precise estimates of the source spectrum and radiation pattern, the effects of 3-D focusing and defocusing, and the effects of viscoelastic attenuation and scattering. Accurate measurement of the decay rate of PKP-Cdiff into the shadow of the inner core boundary must overcome a scatter in measurements similarly induced by lateral variations in focusing, scattering, and attenuation in the mantle and perhaps the lowermost outer core itself.

Perhaps the most robust pointer to a high viscosity at the bottom of the outer core is still its reduced P velocity gradient, which is difficult to explain without appealing to the existence of a chemical boundary layer. The global character of this layer is consistent with it having both higher density and higher viscosity. Observations of large-scale lateral heterogeneity in this layer suggest it may record lateral variation in the solidification process of the inner core and flow near the bottom of the liquid outer core.

ACKNOWLEDGMENTS. This research was supported by grant EAR 07-38492 from the National Science Foundation. The author is grateful for discussions in the ICB group of the 2008 CIDER workshop, which inspired the ideas in this work.

## REFERENCES

- Anderson, D.L., 1989. *Theory of the Earth*, Ch. 14 Anelasticity, pp. 279-302, Blackwell.
- Aubert, J., Amit, H., Hulot, G. & Olson, P., 2008. Thermochemical flows couple the Earth's inner core growth to mantle heterogeneity, *Nature*, **454**, 758–761.
- Bergman, M.I., Macleod-Silberstein, M., Haskel, M., Chandler, B., and Akpan, N., 2005. A laboratory model for the solidification of Earth's core, *Phys. Earth Planet. Int.*, **153**, 150-164.
- Brazhkin, V.V., & Lyapin, A.G., 2000. Universal viscosity growth in metallic melts at megabar pressures: the vitreous state of the Earth's inner core, *Physics-Uspekhi*, **43**, 493-508.
- Cormier, V.F., & Richards, P.G., 1976. Comments on "The Damping of Core Waves" by Anthony Qamar and Alfredo Eisenberg, *J. Geophys. Res.*, **81**, 3066-3068.
- Cormier, V.F. , 1981. Short period PKP and the anelastic mechanism of the inner core, *Phys. Earth Planet Int.*, **24**, 291-301.
- Cormier, V.F., & Richards, P.G., 1988. Spectral synthesis of body waves in Earth models specified by vertically varying layers, In: *Seismological Algorithms*, D. Doornbos (ed.), Academic Press, pp. 3-45.
- Cormier, V.F. , 2007. Texture of the uppermost inner core from forward and back scattered seismic waves, *Earth Planet. Sci. Lett.*, **258**, 442-453, doi: 10.1016/j.epsl.2007.04.003.
- de Wijs, G.A., Kresse, G., Vocadlo, L., Dobson, D. , Alfè, D., Gillan, M.J., & Price, G.D., 1998. The viscosity of liquid iron under Earth's core conditions, *Nature*, **392** , 805-807
- Dziewonski, A.M., & Anderson, D.L., 1981. Preliminary reference Earth model, *Phys. Earth and Planet. Int.* **25**, S.297–356 (1981)

Gubbins, D., Masters, G, Nimmo, F., 2008. A thermochemical boundary layer at the base of Earth's outer core and independent estimate of core heat flux, *Geophys. J. Int.*, **174**, 1007-1018.

Krasnoshchekov, D. N., Kaazik, P.B., & Ovtchinnikov, V.M., 2005. Seismological evidence for mosaic structure of the surface of the Earth's inner core, *Nature*, **435**, 483– 487.

Leyton F., & Koper, K.D., 2007. Using PKiKP coda to determine inner core structure: 2. Determination of Q C, *J. Geophys. Res.*, **112**, B05317, doi:10.1029/2006JB004370.

Okubo, M., Slichter mode (inner core oscillations) detected by Fourier strain analysis, 2009. (abstract), *35<sup>th</sup> IASPEI General Assembly*, Capetown, South Africa.

Palmer, A., & Smylie, D.E., 2005. VLBI observations of free core nutations and viscosity at the top of the core, *Phys. Earth, Planet Int.*, **148**, 285-301, doi: 10.1016/j.pepi.2004.09.0032005

Rudiger, G., & Hollerbach, G., 2004. *The Magnetic Universe: Geophysical and Astrophysical Dynamo Theory*, pp.38-40, Wiley-VCH.

Sato, Y., 1964. Soft core spectrum splitting of the torsional oscillation of an elastic sphere and related problems, *Bull. Earthq. Res. Inst.*, **42**, 1–10.

Schroter , K., G. Wilde, R. Wilnecker, Mweiss, K. Samwer, and E. Donth, 1998. Shear modulus and compliance in the range of the dynamic transition for metallic glasses, *Eur. Phys. J. B.* **5**, pp.1-5, 1998.

Slichter, L.B., 1961. The fundamental free mode of the Earth's inner core, *Science*, **47**, 186-190.

Smylie, D.E., Viscosity near Earth's solid inner core, 1999. *Science*, **284**, 461-463.

Smylie, D.E., Brazhkin, V.V., & Palmer, A., 2009. Direct observations of the viscosity of the outer core and extrapolation of measurements of the viscosity of liquid iron, *Physics-Uspekhi*, **179**, 91-105.

Song, X.D., & Helmberger, D.V., 1995. A P wave velocity model of Earth's core, *J. Geophys. Res.*, **97**, 6573-6586.

Stevenson, D. , 1983., Anomalous bulk viscosity of two-phase fluids and implications for planetary interiors, *J. Geophys. Res.*, **88**, 2445-2455.

Stroujkova, A., & Cormier, V. F., 2004. Regional variations in the uppermost 100 km of the Earth's inner core, *J. Geophys. Res.*, **109**, doi: 10.129/2004JB002976.

Tkalcic, H., Kennett, B.L.N., & Cormier, V.F., 2009. On the inner-outer core density contrast From new PKiKP/PcP amplitude ratios and uncertainties caused by seismic noise, *Geophys. J., Int.*, submitted.

Tsuboi, S., & Saito, M., 2002. Existence of finite rigidity layer at the base of Earth's liquid outer core inferred from anomalous splitting of normal modes, *Earth Planets Space*, **54**, 167-171.

Wilhelm, C., Elias, F., Browaeys, J., Ponton, A., & Bacri, J.C., 2002. Local rheological probes for complex fluids: application to Laponite suspensions, *Phys. Rev.*, **66**, doi:10.1103/PhysRevE.66.021502

Yu, W., Wen, L., & Niu, F., 2005. Seismic velocity structure in the Earth's outer core, *J. Geophys. Res.*, **110**, doi:10.1029/2003JB002928.

Zhang, B., Bai, H.Y., Wang, R.J., Wu, Y., Wang, W.H., Shear modulus as a dominant parameter in glass transitions: Ultrasonic measurement of the temperature dependence of elastic properties of glasses, 2007. *Phys. Rev. B*, **76**, doi:10.1103/PhysRevB.76.012301.

Zou, Z., Koper, K., & Cormier, V.F., 2008. The structure of the base of the outer core inferred from seismic waves diffracted around the inner core, *J. Geophys. Res.*, **113**, doi:10.1029/2007JB005316.

## FIGURE CAPTIONS

Figure 1. Ray paths of PKiKP and PcP and the PKiKP/PcP amplitude ratio predicted by PREM and PREM modified by a non-zero shear velocity of 3.5 km/sec (rigid) and 0.5 km/sec (soft) in the lowermost outer core. Measured PKiKP/PcP amplitude ratios and error bars are from the study by Tkalcic et al. (2008).

Figure 2. Absolute PKiKP amplitudes and estimated error bars measured by Krasnoscheskov et al. (2005). Predicted PKiKP amplitudes by PREM and PREM modified by a non-zero shear velocity of 3.5 km/sec (rigid) and 0.5 km/sec (soft) in the lowermost outer core.

Figure 3. Shear velocity as a function of frequency for two different models of viscosity and in the lowermost outer core, assuming the rheology given by equation (1). Both  $\eta = 10^9$  and  $\eta = 10^{11}$  models fit an upper bound to shear velocity of 0.5 km/sec at 1 Hz in the lowermost outer core constrained from short period observations of PKiKP. The  $h = 109$  model fits the prediction of  $V_s = 0.0015$  km/sec in the lowermost 50 km of the outer core from Tsuboi and Saito's (2002) observation of the  ${}_1S_3$  mode.

Figure 4. The viscoelastic attenuation factor predicted for compressional waves in the lowermost outer core from the  $\eta = 10^9$  and  $\eta = 10^{11}$  viscosity models.

Figure 5. Narrow band filtered seismograms synthesized for body waves interacting with the uppermost inner core from PREM (left) and PREM modified by a lowermost outer core having  $V_s = 3.5$  km/sec at 1 Hz (right).

Figure 6. PKP-Cdiff/PKiKP amplitude ratios measured by Zou et al. (2008) and the predictions of several models of  $V_p$ ,  $V_s$ , and their gradients in the lowermost outer core.

Figure 7. Models of  $V_p$  velocity structure in the lowermost outer core.

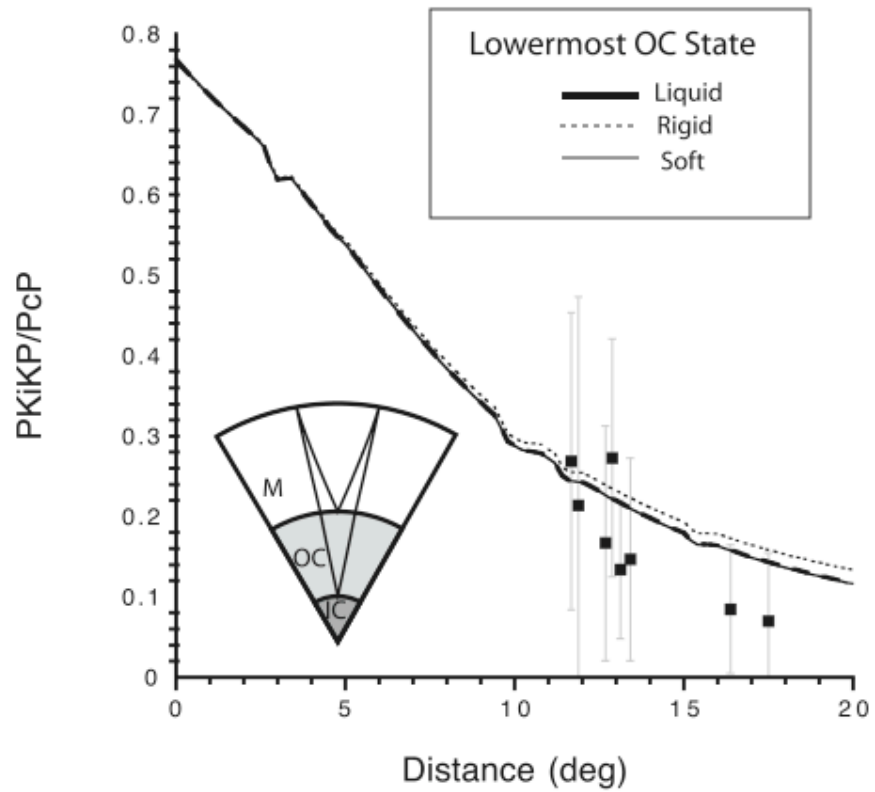


Figure 1

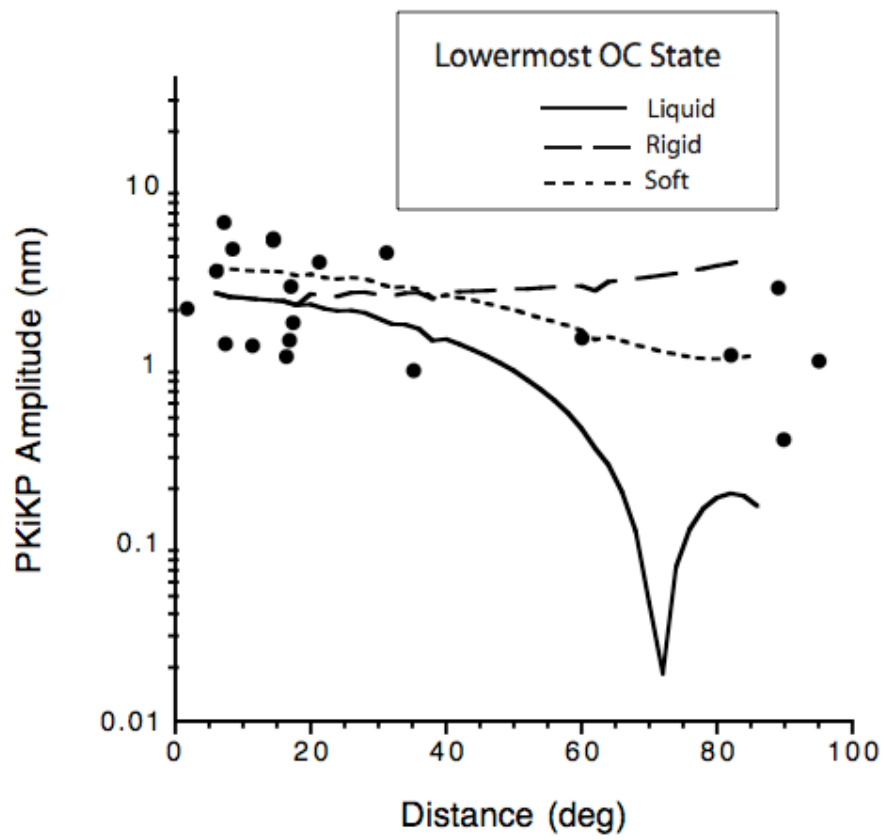


Figure 2

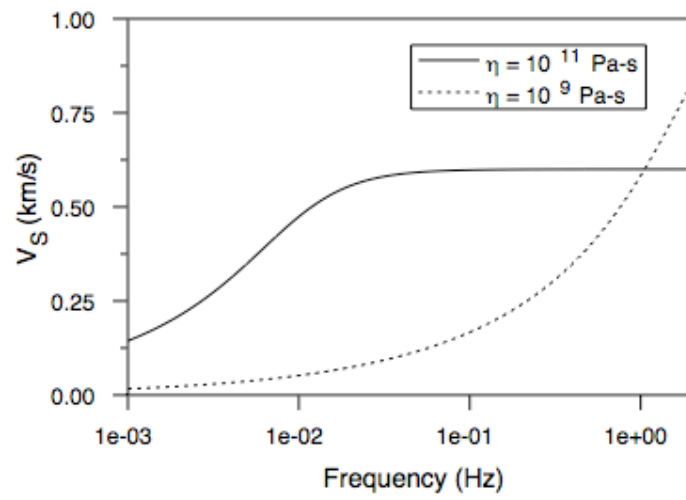


Figure 3

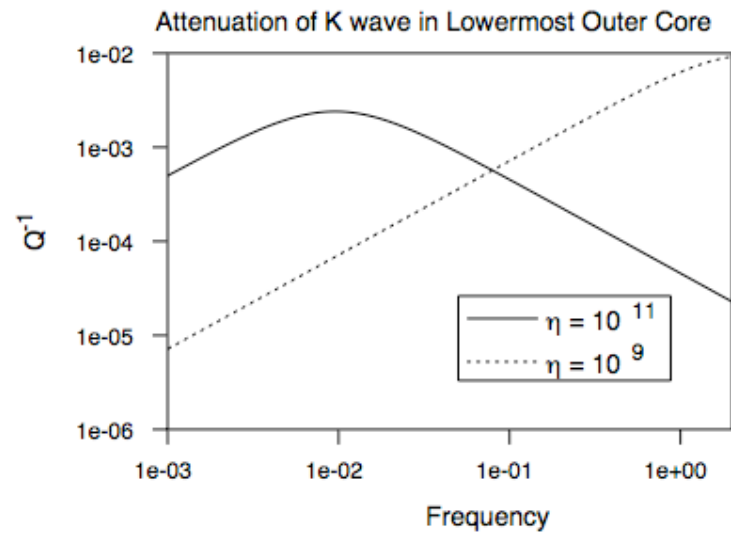


Figure 4

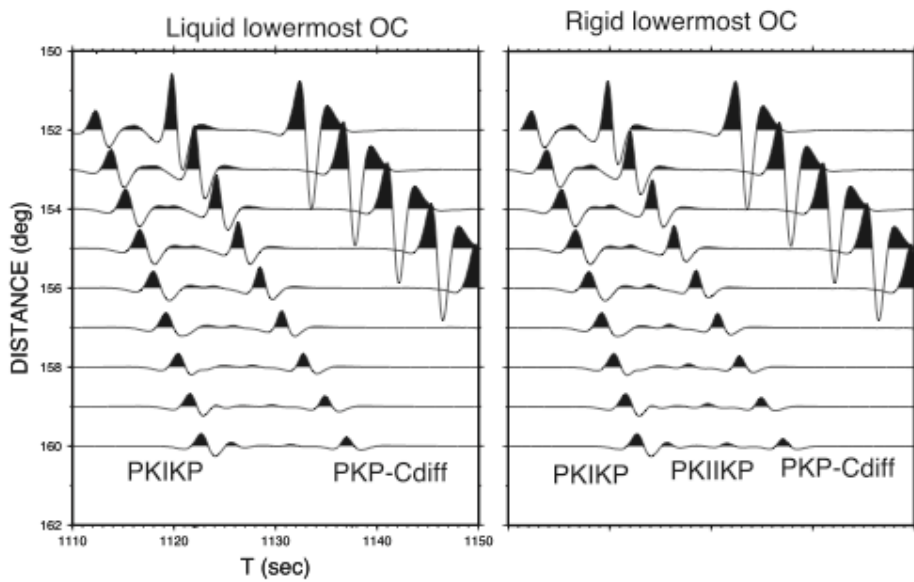


Figure 5

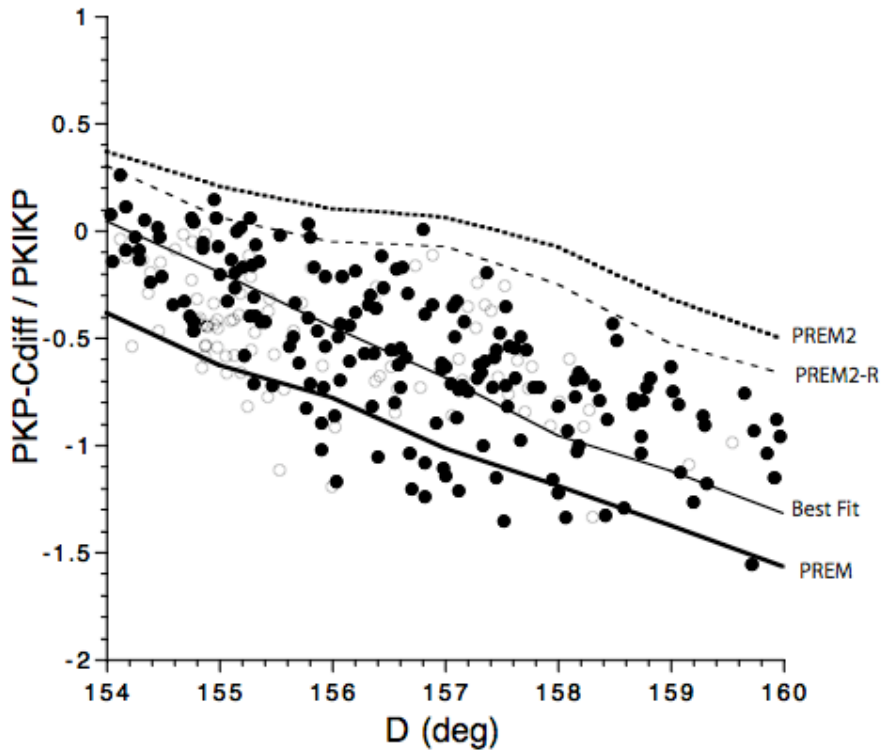


Figure 6

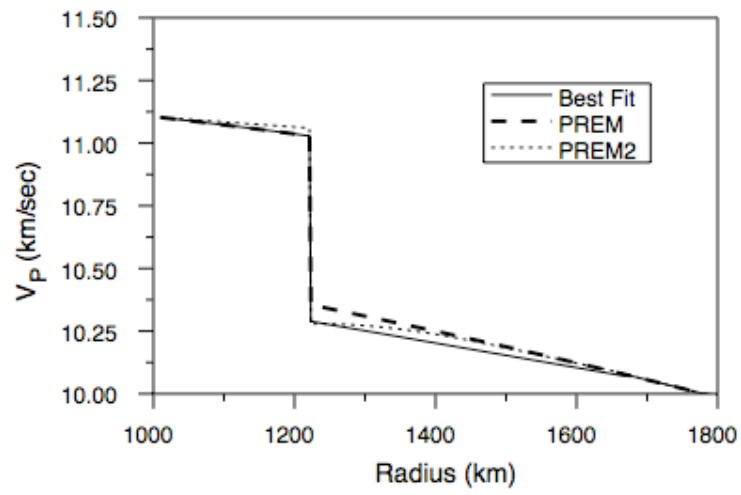


Figure 7